Quantum coherence and spin nematic to nematic quantum phase transitions in biquadratic spin-1 and spin-2 XY chains with rhombic single-ion anisotropy

Rui Mao, Yan-Wei Dai, Sam Young Cho [●],[*] and Huan-Qiang Zhou

Centre for Modern Physics and Department of Physics, Chongqing University, Chongqing 400044, China

We investigate quantum phase transitions and quantum coherence in infinite biquadratic spin-1 and -2 XY chains with rhombic single-ion anisotropy. All considered coherence measures such as the l_1 norm of coherence, the relative entropy of coherence, and the quantum Jensen-Shannon divergence, and the quantum mutual information show consistently that singular behaviors occur for the spin-1 system, which enables to identify quantum phase transitions. For the spin-2 system, the relative entropy of coherence and the quantum mutual information properly detect no singular behavior in the whole system parameter range, while the l_1 norm of coherence and the quantum Jensen-Shannon divergence show a conflicting singular behavior of their first-order derivatives. Examining local magnetic moments and spin quadrupole moments lead to the explicit identification of novel orderings of spin quadrupole moments with zero magnetic moments in the whole parameter space. We find the three uniaxial spin nematic quadrupole phases for the spin-1 system and the two biaxial spin nematic phases for the spin-2 system. For the spin-2 system, the two orthogonal biaxial spin nematic states are connected adiabatically without an explicit phase transition, which can be called quantum crossover. The quantum crossover region is estimated by using the quantum fidelity. Whereas for the spin-1 system, the two discontinuous quantum phase transitions occur between three distinct uniaxial spin nematic phases. We discuss the quantum coherence measures and the quantum mutual information in connection with the quantum phase transitions including the quantum crossover.

I. INTRODUCTION

Quantum phase transitions [1] lie at the heart of quantum many-body phenomena in condensed matter physics. In contrast to classical phase transitions induced by thermal fluctuations, quantum fluctuations originated from the Heisenberg uncertainty principle give rise to quantum phase transitions for varying system parameters at zero temperature. Especially, the investigations of various quantum spin systems have revealed many novel states and quantum phase transitions for quantum magnetism [2]. Of particular interest are quantum nonmagnetic phases of matter such as, for instance, Haldane phase [3–8], dimerized phase [9–12], and spin nematic (or quadrupolar) phase [13–29] because quantum magnetism normally originates from the spin exchange coupling between quantum spins but such exotic states have no conventional long-range magnetic order, i.e., spin correlations are short ranged. Furthermore, in manipulating cold atoms in optical lattice, the recent impressive progresses [30–34] have made various quantum spin nematics [35–41] realizable among other exotic states experimentally.

Essentially, quantum phase transitions are abrupt changes of ground-state wave-function structure driven by quantum fluctuations. Such changes of ground-state wave-function structure lead to similar sudden changes of correlations. For example, in the ground state of the transverse-field Ising

model at zero temperature, the spin-spin correlation is long ranged, indicating the spin ordering, but this disappears exponentially when the transverse field exceeds the critical value [42]. Thus, quantum phase transitions are often characterized by such a behavior of the responsible correlation. Studying the decay of two-point correlation with distance is one of the traditional approaches to investigate quantum phase transition. Meanwhile, quantum correlation measures, introduced from the perspective of information theory, have been shown to be very useful in exploring the states of many-body systems. If it is not known *a priori* whether there is a quantum phase transition or what kind of phase there is at all for a given many-body system, for instance, quantum mutual information measuring the sum of quantum and classical correlations can be used to identify quantum phase transitions [43–49] because the two-point mutual information is bounded from below by any possible two-point correlation in the model [43].

Recent quantification of quantum coherence [50] in quantum information science has also lead to disclose intriguing connections between quantum coherence and correlation [51–54]. Another aspect of fundamental feature of quantum phases and quantum phase transition in a many-body system can be thus explored from a perspective of quantum coherence as a fundamental property of quantum mechanics. Quantum coherence exhibits even in separable product states [55] without quantum entanglement (correlation) [56], which may imply that quantum coherence measures can detect quantum phase transitions even when entanglement measures fail to do so [57]. Actually, a variety of quantum coherence

*sycho@cqu.edu.cn

measures are introduced including the l_1 norm of coherence [50], the relative entropy of coherence [50], and the quantum Jensen-Shannon divergence [58]. Such various quantum coherence measures have been studied in detecting and characterizing quantum phase transitions for several spin chain models such as the transverse-field Ising model [59], the spin-1/2 anisotropic XY chain [60], the two-dimensional Kitaev honeycomb model [61], the anisotropic spin-1/2 Heisenberg XYZ chain with the Dzyaloshinskii-Moriya (DM) interaction in magnetic fields [62,63], the spin-1/2 XY chain with DM interaction under magnetic fields [58], the spin-1/2 XY model with three-spin interaction [64,65] and a transverse magnetic field [66], the compass chain under an alternating magnetic field [55], and the spin-1 XXZ chain [57,67] and bilinear-biquadratic chain [67]. Accordingly, as an example, the continuous (or second-order) quantum phase transition belonging to the Ising universality class in the spin-1/2 XY model has been shown to be captured by using quantum coherence measures such as the derivative of quantum coherence quantified by the l_1 norm of coherence [64], the relative entropy [59], the quantum Jensen-Shannon divergence [58], and the skew information [60].

In fact, many of such studies on quantum coherence in quantum spin systems have been performed for spin-1/2 systems based on available analytical solutions. Higher-spin systems have then received relatively less attention on exploring connections between quantum coherence and quantum phase transitions. In contrast with spin-1/2 systems, however, it is known that the presence of biquadratic interaction can induce a quadrupole order for spins higher than 1/2 [13]. For example, the Heisenberg model with biquadratic interaction possesses a quadrupole phase in two-dimensional spin lattice systems for spin-1 [20,25–28,68–71] and for spin-3/2 [29], and in three-dimensional spin lattices for spin-1 [24].

Thus to understand various aspect of fundamental features of quantum phase transitions, the purpose of this paper is to investigate quantum coherence and quantum phase transition in spin nematic systems without the conventional long-range magnetic order. Specifically, the pure biquadratic spin-1 model $H_{BQ} = J \sum_i (\sum_\alpha S_i^\alpha S_{i+1}^\alpha)^2$ is not in a spin nematic state, where S_i^α is the spin-1 operator at site i and $\alpha \in \{x, y, z\}$. It is well known that the pure biquadratic spin-1 model is in a dimerized state for the interaction strength $J < 0$ [9,10] and in a ferromagnetic state for $J > 0$ [72]. In our study, we then introduce one-dimensional infinite biquadratic spin-1 and spin-2 XY models with rhombic single-ion anisotropy. The main motivation for introducing this model is twofold. On the one hand, we consider the model to search for spin nematic to nematic transitions because at least, to our best knowledge, the full phase diagram of our model is unknown although the rhombic single-ion anisotropy itself gives rise to a spin nematic state for spin-1 system [73,74].

On the other hand, by interpreting the behaviors of quantum information theoretical measures without knowing any information of the full phase diagram of the model, we want to directly demonstrate how and to what extent quantum phase transitions can be understood.

To investigate our infinite-lattice model numerically, we employ the infinite matrix product state (iMPS) representation

with the infinite time-evolving block decimation (iTEBD) method [75–77]. Our numerical results show that the phase diagrams of the spin-1 and -2 systems are very different from each other. Connections between quantum phase transitions and tools of quantum information theory are studied for our spin models by calculating the l_1 norm of coherence, the relative entropy of coherence, the quantum Jensen-Shannon divergence, and the quantum mutual information. The quantum coherence measures show their characteristic features that are the two discontinuities for the spin-1 system and the incoherent point of zero coherence for the spin-2 system. However, in their first-order derivatives at the incoherent point for the spin-2 system, the relative entropy of coherence exhibits a nonsingular behavior, while the l_1 norm of coherence and the quantum Jensen-Shannon divergence have a singular behavior conflictingly. Supportively to the relative entropy of coherence, the quantum mutual information show the two discontinuous jumps for the spin-1 system and the monotonous hill shape without any singular behavior for the spin-2 system. Also, the ground-state energy per site reveals the characteristic features indicating a first-order quantum phase transition for the spin-1 system. For the spin-2 system, the frist- and the second-order derivatives of the ground-state energy per site do not show any nonanalytical feature of the ground-state energy per site indicating quantum phase transition at the corresponding zero coherence point. We find that for the spin-1 system, the local quadrupole order parameters reveal the three quadrupolar ordered phases and exhibit the discontinuous quantum phase transitions between the three distinct uniaxial spin nematic phases in agreement with the results of the tools of quantum information theory. While for the spin-2 system, the two biaxial spin nematic states are connected adiabatically without explicit phase transition at a specific parameter in spite of the orthogonal nematic states, which can be called quantum crossover. The quantum coherence measures and the quantum mutual information are discussed in connection with the quantum crossover.

This paper is organized as follows. In Sec. II, the infinite biquadratic XY chains with rhombic single-ion anisotropy is introduced for spin 1 and 2. A brief explanation of the iMPS approach is given in calculating ground-state wave functions for the infinite chain models. Section III devotes to discuss the behaviors of the quantum coherence measures and the quantum mutual information. To clarify the relationship between quantum phase transitions and quantum coherence measures, we consider the ground-state energy per site and the bipartite entanglement entropy in our iMPS approach in Sec. IV. In Sec. V, the local magnetization and the local quadrupole order parameters are discussed to clarify the uniaxial and biaxial spin nematic phases and the quantum phase transitions in association with the quantum coherence measures and the quantum mutual information. The detailed behaviors of the uniaxial and biaxial spin nematic states are discussed for the spin-1 and -2 systems. A summary and remarks of this work is given in Sec. VI.

In Appendix A, we discuss the iMPS ground-state energy as a function of the truncation dimension. Using the exact diagonalization, as an alternative numerical method, the ground-state energy and the local quadrupole order parame-

ters are shown to be in agreement with the results of the iMPS approach in Appendix B.

II. BIQUADRATIC XY CHAINS AND iMPS APPROACH

We start with the one-dimensional biquadratic spin XY models with rhombic single-ion anisotropy. The Hamiltonian can be written as

$$H = -J \sum_{i=-\infty}^{\infty} \left(S_i^x S_{i+1}^x + S_i^y S_{i+1}^y \right)^2 + R \sum_{i=-\infty}^{\infty} \left[\left(S_i^x \right)^2 - \left(S_i^y \right)^2 \right],$$
(1)

where $J(> 0)$ is the biquadratic exchange interaction and S_i^α is the spin-1 or -2 operator on the ith site. The rhombic single-ion anisotropy is denoted by R, which is normally referred to as zero-field splitting parameter due to a crystal-field anisotropy. The rhombic single-ion anisotropy effect has been very recently investigated in the spin-1 Heisenberg model [73] and XXZ model [74]. We will study the same form of the Hamiltonian (1) for the spin-1 and -2 systems, respectively.

For our one-dimensional infinite lattices of the spin chains, a wave function $|\psi\rangle$ of the Hamiltonian can be represented in the iMPS. By employing the iTEBD method, a numerical ground state $|\psi_G\rangle$ can be obtained in the iMPS representation [77–80]. When the initially chosen state approaches to a ground state, the time step is chosen to decrease from $dt = 0.1$ to $dt = 10^{-6}$ according to a power law. Once the system energy converges to a ground-state energy, which yields a ground-state wave function in the iMPS representation for a given truncation dimension, i.e., here $\chi = 30$. The iMPS ground-state wave function $|\psi_G\rangle$ is the full description of the ground state in a pure state. The full density matrix $\varrho_G = |\psi_G\rangle\langle\psi_G|$ gives any reduced density matrix ϱ_L for lattice-block L by tracing out the degrees of freedom of the rest of the lattice-block L, i.e., $\varrho_L = \text{Tr}_{L^c} \varrho_G$. In our study, single-site reduced density matrix in the S^z basis is used because the reduced density matrices for lattice blocks give no significant changes of the values of quantum coherence measures compared with the single-site coherence measures. The single-spin coherence can be experimentally accessible without requirements of full tomography of the state. For quantum mutual information, two-site reduced density matrix in the S^z basis is used.

III. QUANTUM COHERENCE MEASURES, QUANTUM MUTUAL INFORMATION, AND QUANTUM PHASE TRANSITION

Over the past two decades, quantum information science has developed to embody quantum physical phenomena in quantum information resources that can be exploited to achieve tasks that are beyond the realms of classical physics. Such developments have led to provide quantitative measures for quantum coherence and correlation. The qualitative measures have been implemented to explore another aspects of nature of critical phenomena in quantum many-body systems. In particular, quantum coherence measures and quantum mutual information have been investigated whether they can capture quantum phase transition and its criticality. Also, a nontrivial ground state such as factorized state or product

state has been studied by using such quantum information theoretical measures. Various quantum coherence measures, including the relative entropy of coherence, the l_1 norm quantum coherence, and the Jensen-Shannon divergence, are suggested in different notions of incoherent operations. In our spin chain models, we investigate such quantum coherence measures provided in the alternative frameworks for characterizing quantum phase transitions.

A. Quantum coherence measures

Once a reduced density matrix ϱ is obtained from iMPS ground-state wave functions, one can calculate quantum coherence measures based on the reduced density matrix. For comparison, we consider the three coherence measures, i.e., the l_1 norm of coherence $C_{l_1}(\varrho)$ [50], the relative entropy of coherence $C_{re}(\varrho)$ [50], and the quantum Jensen-Shannon divergence $C_{JS}(\varrho)$ [58]. As a geometric measure that can be used as a formal distance measure, the l_1 norm of coherence $C_{l_1}(\varrho)$ is given as the sum of absolute values of all off-diagonal elements of the density matrix ϱ, i.e.,

$$C_{l_1}(\varrho) = \sum_{n \neq m} |\varrho_{nm}|.$$
(2)

For a given basis, as a valid measure of coherence, the relative entropy of coherence $C_{re}(\varrho)$ is given by

$$C_{re}(\varrho) = S(\varrho \parallel \varrho_{\text{diag}}) = S(\varrho_{\text{diag}}) - S(\varrho),$$
(3)

where removing all off-diagonal entries of ϱ gives the incoherent state ϱ_{diag} corresponding to the state ϱ. $S(\varrho) = -\text{Tr}\varrho \log_2 \varrho$ is the von Neumann entropy. Together with these two coherence measures, we also consider the quantum Jensen-Shannon divergence given as

$$C_{JS}(\varrho) = \sqrt{S\left(\frac{\varrho_{\text{diag}} + \varrho}{2}\right) - \frac{S(\varrho_{\text{diag}}) + S(\varrho)}{2}}.$$
(4)

In our study, the quantum coherence measures are calculated in the S^z basis.

We plot the three coherence measures as a function of R/J for the biquadratic XY chains with rhombic single-ion anisotropy in Fig. 1. For the spin-1 system, Fig. 1(a) shows that all three coherence measures undergo two abrupt jumps at $R = \pm 0.826J \equiv \pm R_c$. These nonanalytical points indicate that discontinuous phase transitions occur at the two points. Furthermore, three coherence measures become zero simultaneously, i.e., $C_{l_1} = C_{re} = C_{JS} = 0$ for $-R_c < R < R_c$. Then the ground state is in an incoherent state for $-R_c < R < R_c$.

In contrast to the case of the spin-1 system, however, Fig. 1(b) shows that the three coherence measures exhibits no such abrupt jumps for the spin-2 system. At $R/J = 0$, the three coherence measures are zero simultaneously and thus the ground state is in an incoherence state. Only the noticeable inflexion of the three coherence measures occurs at $R/J = 0$. In order to confirm whether the incoherent point $R/J = 0$ relates to a quantum phase transition, we perform the numerical derivatives of the three coherence measures. As shown in Fig. 2(a), the first-order derivatives of the C_{l_1} and C_{JS} show their nonanalytical behaviors at $R/J = 0$, which may indicate an occurrence of quantum phase transition, while the relative entropy of coherence C_{re} shows a monotonous change
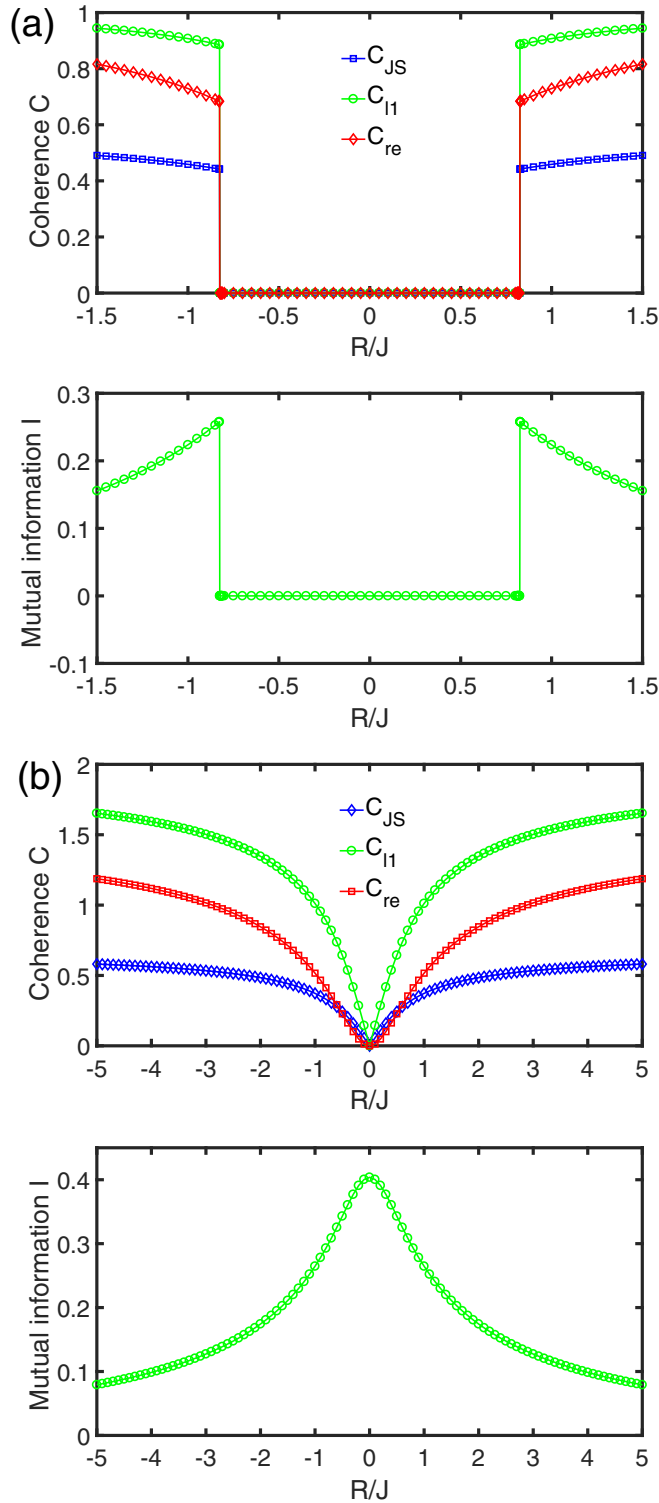
FIG. 1. Quantum coherence measures and quantum mutual information as a function of R/J for (a) the spin-1 system and (b) the spin-2 system.

FIG. 2. First-order derivative of (a) three quantum coherence measures C and (b) quantum mutual information I as a function of R/J for the spin-2 system. In the insets of (a) and (b), the second-order derivatives of the relative entropy of coherence and the quantum mutual information are plotted, respectively.

across the incoherent point. Even the second-order derivative of the C_{re} does not reveal any radical change indicating the nonanalyticity of C_{re}, as shown in the inset of Fig. 2(a).

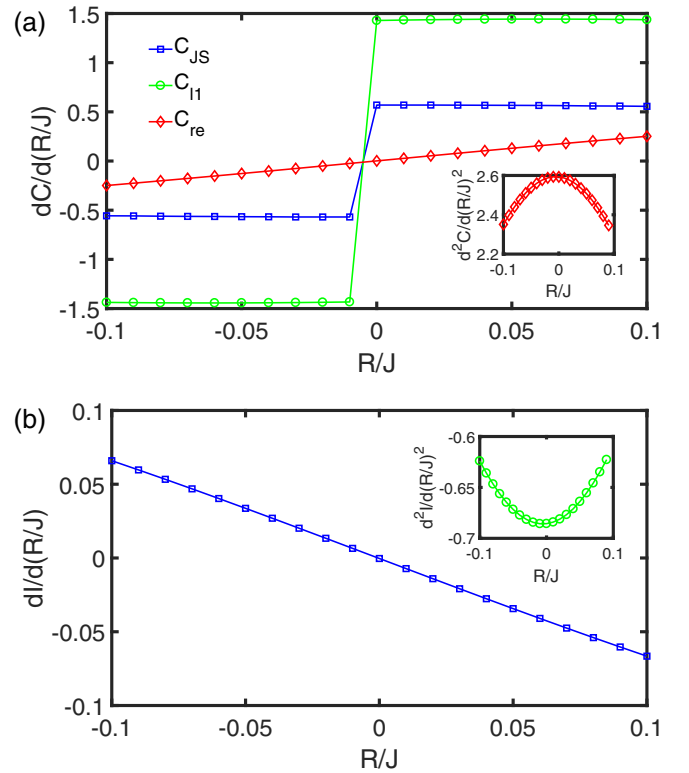At this stage, for the spin-2 system, it cannot be determined whether any quantum phase transition occurs or not

because the nonanalyticity of the C_{re} cannot be determined at $R/J = 0$ up to the second-order derivative of the C_{re}. The other reason is why simply we cannot rule out a possibility of occurring a higher-order quantum phase transition such as, for instance, a Berezinskii-Kosterlitz-Thouless- (BKT) type quantum phase transition known as an infinite-order quantum phase transition [55,58,65] because actually the nonanalyticity of the quantum information theoretic quantities defined by the reduced density matrices is connected to the nonanalyticity of the ground-state energies of quantum many-body systems through the reduced density matrix and its derivatives [81]. Thus from our results at $R/J = 0$, it is hard to determine whether the C_{re} is nonanalytic or not because numerically reaching to a reliable much higher derivative is to be a very difficult task. This issue will then be clarified in the following sections.

Finally, for the both spin-1 and 2 systems in Fig. 1, one can notice that the l_1 norm of coherence $C_{l_1}(\varrho)$ is bigger than the relative entropy of coherence $C_{re}(\varrho)$ except for that all coherence measures are zero in the range of $-R_c < R < R_c$ for the spin-1 system and at the incoherent point $R/J = 0$ for the spin-2 system. This implies that $C_{l_1}(\varrho) \geqslant C_{re}(\varrho)$ holds, which was conjectured and proved only for the pure states and qubit states in Ref. [82]. For a mixed state, the validity of the conjecture was shown in a compass chain under an alternating magnetic field in Ref. [55]. Thus our result support that the l_1 norm of coherence $C_{l_1}(\varrho)$ is an upper bound for the

relative entropy of coherence $C_{re}(\varrho)$, i.e., $C_{l_1}(\varrho) \geqslant C_{re}(\varrho)$ for our mixed states.

B. Quantum mutual information

In the previous subsection, we have studied the quantum coherence measures in detecting quantum phase transitions. Interestingly, the spin-2 system exhibits an inconsistent behavior on the quantum coherence measures. At the incoherent point $R/J = 0$, the nonanalytical behaviors of the l_1 norm of coherence [64] and the quantum Jensen-Shannon divergence [58] can be interpreted as an occurrence of quantum phase transition. However, the nonanalyticity of the C_{re} could not be demonstrated. As we discussed in the Introduction, correlations can also undergo an abrupt change for quantum phase transitions. Thus in this subsection, we will consider a generalized correlation, i.e., the quantum mutual information that is based on entanglement entropy and measures a total sum of classical and quantum correlations without knowing a proper correlation operator. Using the von Neumann entropy, the quantum mutual information between two sites A and B can be defined as

$$I(A : B) = S_A + S_B - S_{AB}, \qquad (5)$$

where $S_{A/A \cup B} = -\text{Tr}\varrho_{A/A \cup B} \log_2 \varrho_{A/A \cup B}$ are the von Neumann entropies with the reduced density matrix $\varrho_{A/A \cup B}$ for one site A and two sites $A \cup B$, respectively. This quantum mutual information can be used to detect and characterize quantum phase transitions [44–49].

From our iMPS ground states for the Hamiltonian of Eq. (1), we calculate the quantum mutual information for the adjacent two spins. In Fig. 1(a), the quantum mutual information $I(R/J)$ is plotted as a function of the interaction rate R/J for the spin-1 system. Straightforwardly, one can notice the discontinuous behaviors of the quantum mutual information at the corresponding discontinuous points of the quantum coherence measures. As one may expect, this nonanalytical behavior is consistent with those of all quantum coherence measures. The discontinuous behaviors of all tools of quantum information theory indicate the occurrence of discontinuous quantum phase transitions at the points $R = \pm R_c$. Noticeably, the quantum mutual information vanishes to be zero for $-R_c < R < R_c$. This region of zero quantum mutual information corresponds to that of the incoherent phase for $-R_c < R < R_c$. In the parameter region, the vanishing quantum mutual information means that the entanglement between the adjacent two spins becomes zero. As a result, the ground state is in a product state in the incoherent phase for $-R_c < R < R_c$.

For the spin-2 system, Fig. 1(b) shows a monotonous hill shape of the quantum mutual information that has a maximum value at the incoherent point $R/J = 0$. Interestingly, compared to the incoherent phase of the spin-1 system for $-R_c < R < R_c$, where the entanglement between the adjacent two spins is zero, the incoherent state at $R/J = 0$ for the spin-2 system has a maximum correlation and thus is not a product state. Such a maximum value can indicate a quantum phase transition. We calculate the derivatives of the quantum mutual information to search for a possible nonanalyticity of the quantum mutual information. However, as shown in Fig. 2(b), similarly to the

relative entropy of coherence C_{re} in Fig. 2(a), the first-order and the second-order derivatives of the quantum mutual information shows a monotonous change across the incoherent point $R/J = 0$. Accordingly, similarly to the relative entropy of coherence C_{re}, our quantum mutual information I cannot determine clearly whether a quantum phase transition occurs at the incoherent point. However, it should be noted that although the quantum mutual information I measures a different fundamental nature of ground state from the relative entropy of coherence, it behaves in accordance with the relative entropy of coherence C_{re} in detecting quantum phase transition. In this aspect, it is possible to say that for the spin-2 system, the quantum mutual information I and the relative entropy of coherence C_{re} behave conflictingly to the l_1 norm of coherence C_{l_1} and the quantum Jensen-Shannon divergence C_{JS}. Then we will study the nonanalyticity of ground-state energy to solve this interesting issue in the following section.

IV. GROUND-STATE ENERGY, ENTANGLEMENT ENTROPY, AND QUANTUM PHASE TRANSITION

So far, we have discussed about the behaviors of the tools of quantum information theory in characterizing quantum phase transitions. However, for the spin-2 biquadratic XY chain with rhombic single-ion anisotropy, the quantum coherence measures detect the conflicting behavior each other although the quantum mutual information I is supportive to the relative entropy of coherence C_{re}. As a standard framework, quantum phase transitions are actually connected with the intrinsic features of ground-state energy of the quantum many-body systems, i.e., the energy level crossings which lead to the appearance of nonanalyticities of ground-state energy. Thus we discuss the behaviors of the ground-state energy per site e to resolve the conflicting issue for the spin-2 system in this section.

From our iMPS ground states for the Hamiltonian of Eq. (1), one can calculate the ground-state energy. In Fig. 3, the ground-state energy per site e is plotted as a function of the interaction rate R/J for (a) the spin-1 and (b) spin-2 systems. In the insets, the first- and second-order derivatives of the ground-state energy are also plotted. In Fig. 3(a) for the spin-1 system, the ground-state energy $e(R/J)$ shows clearly the two sharp kinks indicating energy level crossings at $R = \pm R_c$ and the first derivative of the ground-state energy also shows its discontinuities at the same points, which indicates that first-order quantum phase transitions take place. Thus this result manifests that the discontinuities of the three coherence measures and the quantum mutual information in Sec. III detect the occurrences of the first-order (discontinuous) quantum phase transitions at the transition points $R = \pm R_c$.

Contrastively to the spin-1 system, Fig. 3(b) shows that the ground-state energy is monotonous and any noticeable significant change for possible phase transitions around $R/J = 0$ is not seen in the first and second derivatives of the ground-state energy. Then the monotonous behaviors of the ground-state energy could not also solve the conflicting behaviors of the quantum coherence measures, i.e., whether quantum phase transition happens or not at $R/J = 0$ for the spin-2 system. However, it should be noted that the ground-state energy e behaves in accordance with the quantum mutual information I
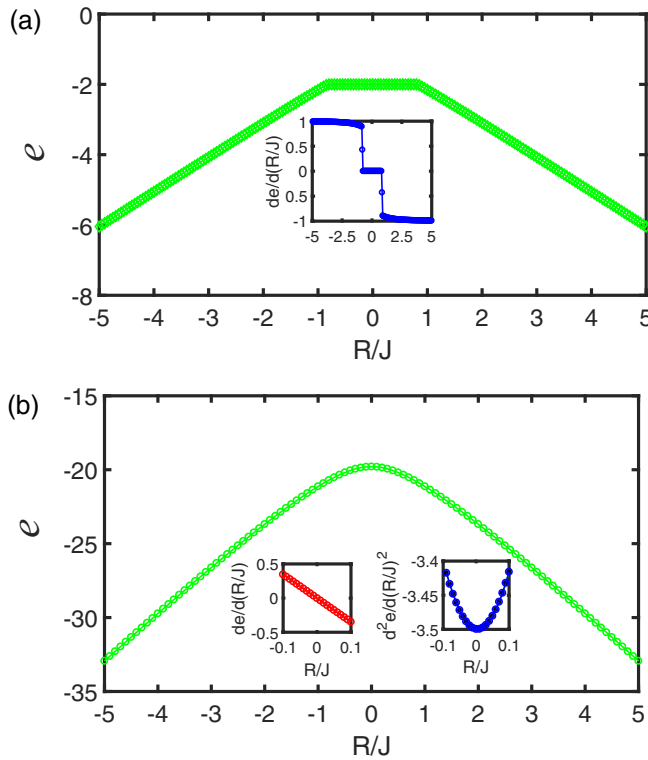
FIG. 3. Ground-state energy per site e as a function of R/J for (a) the spin-1 system and (b) the spin-2 system. In the inset of (a), the first-order derivative of ground-state energy per site is plotted for the spin-1 system. Also, we plot the first- and the second-order derivatives of ground-state energy per site in the inset of (b) for the spin-2 system.

and the relative entropy of coherence C_{re} in detecting quantum phase transitions.

Actually, our iMPS approach provide a way to detecting critical systems by using its characteristic scaling property of bipartite entanglement entropy [77–80,83–87]. In the iMPS approach, it is known that the bipartite entanglement entropy diverges in critical systems as the truncation dimension χ increases. For discontinuous (first-order) phase transitions, the first-order transitions are not critical and thus the bipartite entanglement entropy does not diverge for increment of the truncation dimension. Actually, for the spin-1 system, the bipartite entanglement entropy exhibit discontinuous behaviors at the first-order transitions (the details are not presented here).

In order to get more insight into the conflicting point, let us then consider the bipartite entanglement entropy for the spin-2 system. Thus we calculate the bipartite entanglement entropy (the von Neumann entropy) by considering the bipartitioned two semi-infinite chains in the iMPS representation [77–80]. We plot the bipartite entanglement entropy $S_{vN}(\chi)$ as a function of the truncation dimension χ at $R/J = 0$ in Fig. 4. Usually at critical points for continuous phase transitions, the bipartite entanglement entropy diverges as the truncation dimension χ increases. Figure 4, however, shows clearly that the entanglement entropy does not diverge but converges as the truncation dimension increases. Even the entanglement entropy does not change much with the increase of the trunca-
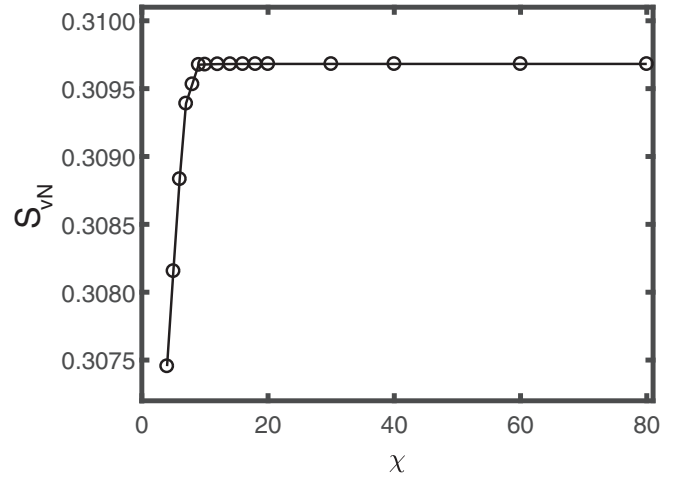

FIG. 4. Bipartite entanglement entropy $S_{vN}(\chi)$ as a function of the truncation dimension χ at the incoherent point $R/J = 0$ for the spin-2 system.

tion dimension for higher truncation dimension than $\chi = 30$. Accordingly, this result clarifies that the ground state is not critical at the incoherent point $R/J = 0$ and then any continuous quantum phase transition across the incoherence point does not take place. Also, a discontinuous phase transition does not occur at $R/J = 0$ because the ground-state energy as well as the quantum mutual information and the relative entropy of coherence is continuous. Conclusively, together with the ground-state energy, the mutual information and the relative entropy of coherence, the result of the bipartite entanglement entropy represents no occurrence of explicit quantum phase transition at $R/J = 0$ for the spin-2 system.

Such a conclusion leaves two consequent unconformable facts. In the aspect of the quantum coherence measures, the nonanalytical behaviors of the l_1 norm of coherence C_{l_1} and the quantum Jensen-Shannon divergence C_{JS} cannot be interpreted as an indication of quantum phase transition at the incoherent point $R/J = 0$ for the spin-2 system. In the viewpoint of quantum phase and quantum phase transition, more intriguing thing is the fact that the incoherent point has nothing to do with any continuous or discontinuous quantum phase transition. This fact that the spin-2 system does not undergo any explicit phase transition implies that the spin-2 system has a very different phase diagram of ground state from the spin-1 system even though they have the same form of the Hamiltonian (1). It shows that spin-2 has fundamentally different nature from spin-1. The essential difference between the spin-1 and -2 systems will become apparent in the phase diagrams in the following section.

V. QUANTUM SPIN NEMATIC PHASE TRANSITIONS

In order to identify the quantum phases in the biquadratic XY chains with rhombic single-ion anisotropy, let us first consider the local magnetizations $\langle S_i^\alpha \rangle$. Existing a local magnetization implies that the individual spins in the chain are oriented in a direction in spin space. Such a spin ordered state is induced by spontaneous breaking both spin-rotation and time-reversal symmetries. Normally, external fields can break such symmetries and can make spins ordered in a

direction. For the both spin-1 and -2 biquadratic XY chains with rhombic single-ion anisotropy, however, we find that all components of magnetization are zero for the whole parameter space, i.e., $\langle S_i^\alpha \rangle = 0$ for the ground states, which implies that all states of our model preserve time-reversal symmetry for the whole parameter space. According to the results of the ground-state energy and the coherence measures, thus our systems can have quantum phases without magnetic order, i.e., the so-called spin nematic phases. According to the results of the quantum coherence measures, the quantum mutual information, and the ground-state energy, quantum phase transitions can occur between spin nematic phases in our spin systems. Behaviors of quadrupole moments will then characterize quantum spin nematic phases of our spin systems.

Let us consider the quadrupole moment measured by products of spin operators. A symmetric and traceless rank-2 quadrupole tensor operator [70,88] can be given by

$$Q_i^{\alpha\beta} = \tfrac{1}{2}\left(S_i^\alpha S_i^\beta + S_i^\beta S_i^\alpha\right) - \tfrac{1}{3}\mathbf{S}_i^2 \delta_{\alpha\beta} \tag{6}$$

with $\alpha, \beta \in \{x, y, z\}$ and the Kronecker delta $\delta_{\alpha\beta}$ at site i. The actual independent components of quadrupole tensor operator are five because $\sum_\alpha Q_i^{\alpha\alpha} = 0$ for $\alpha = \beta$ and $Q^{\alpha\beta} = Q^{\beta\alpha}$ for $\alpha \neq \beta$. We find that all off-diagonal components of quadrupole moments are zero for the whole parameter space, i.e., $\langle Q_i^{xy} \rangle = \langle Q_i^{yz} \rangle = \langle Q_i^{zx} \rangle = 0$ for the both spin-1 and -2 ground states. Thus two actual components of quadrupole tensor operator can identify quantum phases in our spin systems. We calculate the two quadrupole orders given as

$$Q_i^{x^2-y^2} = Q_i^{xx} - Q_i^{yy}, \tag{7}$$

$$Q_i^{3z^2-r^2} = 3Q_i^{zz}. \tag{8}$$

Nonzero quadrupole moments can characterize ground states breaking spin-rotational symmetry by developing an isotropy in their spin fluctuations, which indicates that our spin-1 and spin-2 systems are in spin nematic quadrupole phases.

A. Quadrupole phases for the spin-1 system

Let us first discuss about quadrupole phases in the spin-1 biquadratic XY chain with rhombic single-ion anisotropy. Figure 5 displays $\langle Q_i^{x^2-y^2} \rangle$ and $\langle Q_i^{3z^2-r^2} \rangle$ as a function of R/J for the spin-1 system, which shows clearly the discontinuities of the quandrupole order parameters indicating the occurrence of the first-order quantum phase transitions as the quantum coherence measures and the quantum mutual information detected. In each phase, the quadrupole state can be characterized by the quadrupole moments. We identify the phases with the characterization of the quadrupole moments as follows.

(i) The y-ferroquadrupole phase with $\langle Q_i^{x^2-y^2} \rangle > 0$ for $R < -R_c$. As shown in Fig. 5, $\langle Q_i^{3z^2-r^2} \rangle = 1$, i.e., $\langle Q_i^{zz} \rangle = 1/3$ parameter independently for $R < -R_c$. At large negative R/J, $\langle Q_i^{x^2-y^2} \rangle = \langle Q_i^{3z^2-r^2} \rangle$ gives $\langle Q_i^{xx} \rangle = \langle Q_i^{zz} \rangle = -\tfrac{1}{2}\langle Q_i^{yy} \rangle$, which implies that the ground state is a uniaxial spin nematic state.

In the limit of large negative R/J, the rhombic single-ion anisotropy becomes predominant and thus the local spin state is forced to be the lowest-energy state of the anisotropy term $R[(S_i^y)^2 - (S_i^x)^2]$ in the Hamiltonian (1), which is given by
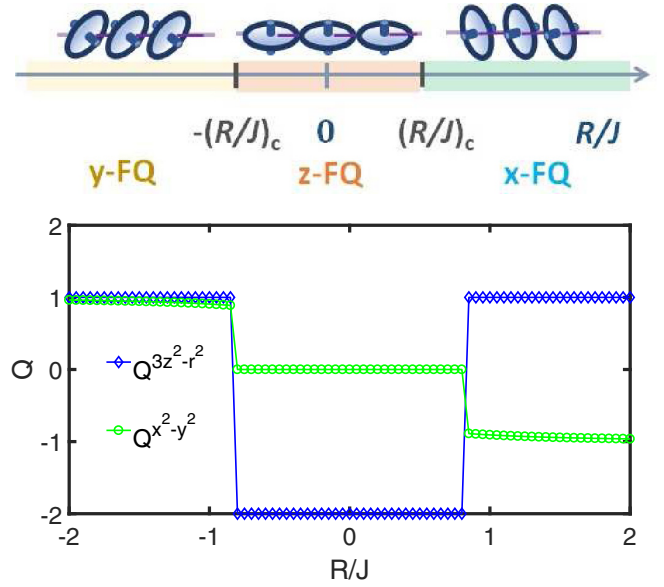

FIG. 5. Top: Schematic phase diagram. Bottom: Quadrupole order parameters $\langle Q^{x^2-y^2} \rangle$ and $\langle Q^{3z^2-r^2} \rangle$ as a function of R/J for the spin-1 system. In the phase diagram, α-FQ denote the ferroquadrupole phases with the zero local spin fluctuation in the α axis ($\alpha \in \{x, y, z\}$). A disk indicates the local spin fluctuation in the plane perpendicular to the α axis at site i [28].

$|S_i^y = 0\rangle$, where the local spin fluctuates in the zx plane [73]. Thus, as shown in the phase diagram in Fig. 5, with the zero local magnetization $S^\alpha = 0$, the local spin fluctuations are like a disk in the zx plane and have zero amplitude along the y axis [28]. Accordingly, this ground state is a uniaxial spin nematic state and the product state of $|S_i^y = 0\rangle$. This phase is referred to as the y-ferroquadrupole phase.

As the negative R/J approaches to the transition point $R = -R_c$ from near $R = -R_c$, a little local spin fluctuation arises along the y axis and decreases the same amount of the local spin fluctuation along the x axis without changing along the z axis because the local spin fluctuation does not change for the y-ferroquadrupole phase, i.e., $\langle (S_i^z)^2 \rangle = 1$. The changes of quadrupole moments reflect to this little local spin fluctuation in the same manner. When the negative R/J crosses the transition point, the first-order quantum phase transition takes place at $R = -R_c$.

(ii) The z-ferroquadrupole phase with $\langle Q_i^{x^2-y^2} \rangle = 0$ for $-R_c < R < R_c$. Figure 5 shows that $\langle Q_i^{3z^2-r^2} \rangle = -2$, i.e., $\langle Q_i^{zz} \rangle = -2/3$ and $\langle Q_i^{x^2-y^2} \rangle = 0$ parameter-independently for $-R_c < R < R_c$. This fact gives $\langle Q_i^{xx} \rangle = \langle Q_i^{yy} \rangle = -\tfrac{1}{2}\langle Q_i^{zz} \rangle$. Straightforwardly, the local spin fluctuations are given as $\langle (S^x)^2 \rangle = \langle (S^y)^2 \rangle = 1$ and $\langle (S^z)^2 \rangle = 0$, which means that the ground state is a uniaxial spin nematic state [14,15]. Thus the local spin fluctuates only in the xy plane, with no change in the z axis for the parameter range of the phase. As noticed in the quantum mutual information, the ground state is in a product state, i.e., the product state of $|S_i^z = 0\rangle$ for the parameter range $-R_c < R < R_c$. Due to the robust local spin fluctuation in the xy plane for the phase, the ground-state structure in the product state does not change until the

rhombic single-ion anisotropy overwhelms the biquadratic interaction to induce the sudden change of the spin fluctuation at the transition points $R = \pm R_c$. This phase is referred to the z-ferroquadrupole phase.

(iii) The x-ferroquadrupole phase with $\langle Q_i^{x^2-y^2} \rangle > 0$ for $R > R_c$. This phase has the constant quadrupole order $\langle Q_i^{3z^2-r^2} \rangle = 1$, i.e., $\langle Q_i^{zz} \rangle = 1/3$. At large positive R/J, as shown in Fig. 5, $\langle Q_i^{x^2-y^2} \rangle = -\langle Q_i^{3z^2-r^2} \rangle = -1$ gives $\langle Q_i^{yy} \rangle = \langle Q_i^{zz} \rangle = -\frac{1}{2}\langle Q_i^{xx} \rangle$, indicating that the ground state is a uniaxial spin nematic state. This positive R/J is equivalent to exchanging the x axis and y axis of the rhombic single-ion anisotropy term $R[(S_i^y)^2 - (S_i^x)^2]$ in the Hamiltonian (1) for the case of the y-ferroquadrupole phase. The local spin state is forced to be the lowest-energy state of the anisotropy term $R[(S_i^x)^2 - (S_i^y)^2]$ in the Hamiltonian, which is given by $|S_i^x = 0\rangle$, where the local spin fluctuates in the yz plane [73]. As a result, the ground state is a uniaxial spin nematic state and the product state of $|S_i^x = 0\rangle$. This phase is referred to as the x-ferroquadrupole phase.

Similarly to the y-ferroqudrupole phase, as the positive R/J approaches to the transition point $R = R_c$ from near $R = R_c$ in the x-ferroquadrupole phase, a little local spin fluctuation arises along the x axis and decreases the same amount of the local spin fluctuation along the y axis without changing along the z axis because the local spin fluctuation does not change for the y-ferroquadrupole phase, i.e., $\langle (S_i^z)^2 \rangle = 1$. When the positive R/J crosses the transition point in the x-ferroquadrupole phase, the first-order quantum phase transition occurs at $R = R_c$.

B. Quantum crossover for the spin-2 system

Next, we study the spin-2 biquadratic XY chain with rhombic single-ion anisotropy. As one can easily notice, the spin-2 quadrupole order parameter $\langle Q_i^{x^2-y^2} \rangle$ in Fig. 6(a) reveals its very different behavior from the discontinuous features of the spin-1 quadrupole order parameter in Fig. 5. Only a noticeable change of the spin-2 quadrupole order parameter $\langle Q_i^{x^2-y^2} \rangle$ is its sign change through $R = 0$. According to the sign of the quadrupole order parameter, the two distinct phases are distinguished. Thus let us discuss in details of the quadrupole order parameter to clarify what kind of phases can exist and whether a phase transition occurs or not.

(i) The positive biaxial spin nematic phase with $\langle Q_i^{x^2-y^2} \rangle > 0$ for $R < 0$. At large negative R/J, $\langle Q_i^{x^2-y^2} \rangle = 2\sqrt{3}$ and $\langle Q_i^{3z^2-r^2} \rangle = 0$ gives $\langle Q_i^{xx} \rangle = -\langle Q_i^{yy} \rangle = \sqrt{3}$ and $\langle Q_i^{zz} \rangle = 0$ [35]. In contrast to the spin-1 system, then the ground state is a biaxial spin nematic state [35]. Similarly to the spin-1 system, in the limit of large negative R/J, the spin-2 rhombic single-ion anisotropy becomes predominant and thus the local spin state is forced to be the lowest-energy state of the rhombic-anisotropy term $R[(S_i^y)^2 - (S_i^x)^2]$ in the Hamiltonian (1). In sharp contrast to the spin-1 system, however, the local spin state is not given by $|S_i^y = 0\rangle$ where the local spin fluctuates in the zx plane for the spin-1 system. Whereas for the spin-2 system, the local spin fluctuates along the all axes and the lowest-energy state gives $\langle (S_i^x)^2 \rangle = 2 + \sqrt{3}$, $\langle (S_i^y)^2 \rangle = 2 - \sqrt{3}$, and $\langle (S_i^z)^2 \rangle = 2$ with $\langle S_i^\alpha \rangle = 0$. Accord-
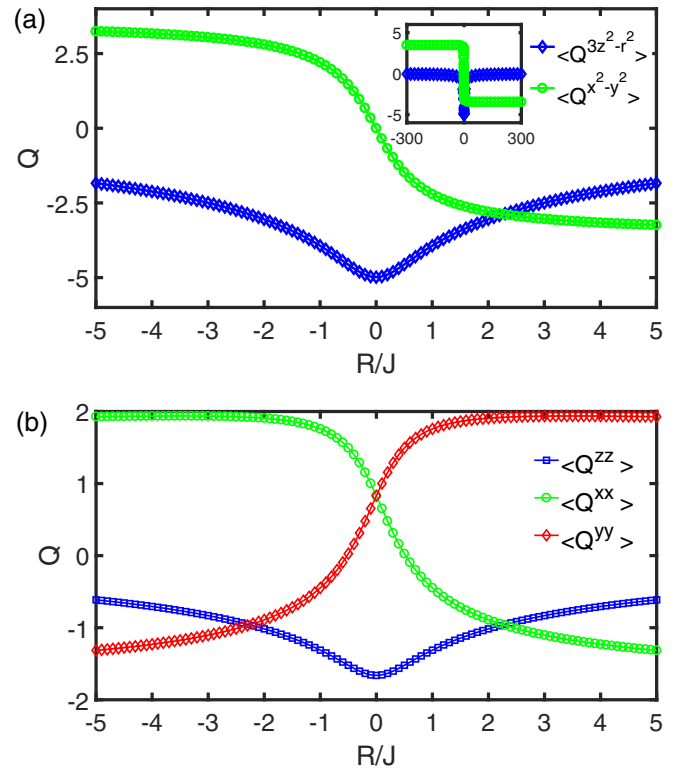

FIG. 6. (a) Quadrupole order parameters $\langle Q^{x^2-y^2} \rangle$ and $\langle Q^{3z^2-r^2} \rangle$ and (b) quadrupole moments $\langle Q^{\alpha\alpha} \rangle$ as a function of R/J for the spin-2 system.

ingly, this ground state is a biaxial spin nematic state and the product state of the lowest-energy state of $R[(S_i^y)^2 - (S_i^x)^2]$ given by $a|S_i^x = 0\rangle + b|S_i^y = 0\rangle$ with $a = (1 + \sqrt{3})/\sqrt{6}$ and $b = (1 - \sqrt{3})/\sqrt{6}$. This phase is then referred to the *positive* biaxial spin nematic phase for the positive order parameter $\langle Q_i^{x^2-y^2} \rangle > 0$.

(ii) The ground state at $R/J = 0$, where $\langle Q_i^{x^2-y^2} \rangle = 0$. $\langle Q_i^{x^2-y^2} \rangle = 0$ gives $\langle Q_i^{xx} \rangle = \langle Q_i^{yy} \rangle = -\frac{1}{2}\langle Q_i^{zz} \rangle > 0$ at $R/J = 0$, as shown in Fig. 6(a). Thus the ground state is not critical and a product state, but it is a uniaxial spin nematic state. However, in contrast to the spin-1 system, the local spin fluctuation is not confined in the xy plane. Actually, this point $R = 0$ corresponds to the maximum fluctuation point of the local spin along the z axis for the whole parameter space, as shown in Fig. 6(b).

In fact, there are two more such uniaxial nematic states. From Fig. 6(b), one can notice that there are the three uniaxial nematic states at $R = 0$, R_a, and $-R_a$ with $R_a = 2.264J$ in the whole parameter space. At $R = -R_a$ and R_a, the quadrupole moments are given as $\langle Q_i^{yy} \rangle = \langle Q_i^{zz} \rangle = -\frac{1}{2}\langle Q_i^{xx} \rangle < 0$ and $\langle Q_i^{zz} \rangle = \langle Q_i^{xx} \rangle = -\frac{1}{2}\langle Q_i^{yy} \rangle < 0$, respectively. For the three uniaxial spin nematic states, as we discussed in the spin-1 system, the local spin fluctuation is confined in a plane.

(iii) The negative biaxial nematic phase with $\langle Q_i^{x^2-y^2} \rangle < 0$ for $R > 0$. Contrary to the large negative R/J, at large positive R/J, $\langle Q_i^{x^2-y^2} \rangle = -2\sqrt{3}$ and $\langle Q_i^{3z^2-r^2} \rangle = 0$ gives $\langle Q_i^{xx} \rangle = -\langle Q_i^{yy} \rangle = \sqrt{3}$ and $\langle Q_i^{zz} \rangle = 0$, i.e., the ground state is a biaxial

spin nematic state. Similarly to the large negative R/J, in the limit of large positive R/J, the rhombic single-ion anisotropy becomes predominant and thus the local spin state is forced to be the lowest-energy state of the rhombic-anisotropy term $R[(S_i^x)^2 - (S_i^y)^2]$ in the Hamiltonian (1). The local spin fluctuates in the all axes and the lowest-energy state gives $\langle (S_i^x)^2 \rangle = 2 - \sqrt{3}$, $\langle (S_i^y)^2 \rangle = 2 + \sqrt{3}$, and $\langle (S_i^z)^2 \rangle = 2$ with $\langle S_i^\alpha \rangle = 0$ as they should be. Accordingly, this ground state is a biaxial spin nematic state and the product state of the lowest-energy state $R[(S_i^x)^2 - (S_i^y)^2]$ given by $b|S_i^x = 0\rangle + a|S_i^y = 0\rangle$. This phase is referred to the *negative* biaxial spin nematic phase for the negative order parameter $\langle Q_i^{x^2 - y^2} \rangle < 0$.

Note that the positive and negative biaxial spin nematic states are orthogonal each other although $|S_i^x = 0\rangle$ and $|S_i^y = 0\rangle$ are not orthogonal each other. Thus depending on the sign of the quadrupole order parameter $\langle Q_i^{x^2 - y^2} \rangle$, the two distinct biaxial spin nematic phases can be distinguished. However, as noticed by the relative entropy of coherence C_{re} and the quantum mutual information I in Sec. III, and the ground-state energy per site e in Sec. IV, the spin-2 biquadratic XY chain with rhombic single-ion anisotropy does not undergo any explicit phase transition as the R/J varies from $R/J = -\infty$ to $R/J = \infty$. Accordingly, the two orthogonal biaxial spin nematic states are connected adiabatically without an explicit abrupt phase transition.

This adiabatic connection between the two orthogonal biaxial spin nematic states can be called *quantum crossover* that is a substantial change in the nature of many-body ground state that occurs over a finite range of the system parameter rather than abruptly at a critical point. This can be understood by comparing with the quantum phase transition between those two biaxial spin nematic states. To do this, let us consider the Hamiltonian in Eq. (1) for $J = 0$, i.e., $H_R = R \sum_{i=-\infty}^{\infty} [(S_i^x)^2 - (S_i^y)^2]$. For $R < 0$, similar to the Hamiltonian in Eq. (1), the ground state is given by the product state of $a|S_i^x = 0\rangle + b|S_i^y = 0\rangle$. While for $R > 0$, the ground state should be the product state of $b|S_i^x = 0\rangle + a|S_i^y = 0\rangle$. The quandrupole order parameter becomes $\langle Q_i^{x^2 - y^2} \rangle = 2\sqrt{3}$ for $R < 0$ and $\langle Q_i^{x^2 - y^2} \rangle = -2\sqrt{3}$ for $R > 0$, where $\langle Q^{3z^2 - r^2} \rangle = 0$. It is shown clearly that the ground state changes abruptly at $R = 0$. The discontinuity of the quadrupole order parameter indicates an occurrence of discontinuous quantum phase transition between the positive and negative biaxial spin nematic phases at $R = 0$. In sharp contrast to this discontinuous quantum phase transition at $R = 0$, as a consequence, the spin-2 biquadratic XY chain with rhombic single-ion anisotropy undergoes the quantum crossover between the two biaxial spin nematic states.

The substantial change of ground-state wave-function structure for the quantum crossover can be quantified by directly comparing the ground-state wave functions. Actually, one can define the overlap function between the ground-state wave functions as, for instance, $f(R/J) = \langle \psi_G(R/J)|\psi_G(+\infty) \rangle$ that ranges $0 \leqslant f(R/J) \leqslant 1$ because the positive and negative biaxial spin nematic states are orthogonal each other, i.e., $\langle \psi_G(-\infty)|\psi_G(+\infty) \rangle = 0$, and the overlap function of the positive/negative biaxial spin nematic states by themselves give $\langle \psi_G(\pm\infty)|\psi_G(\pm\infty) \rangle = 1$, where
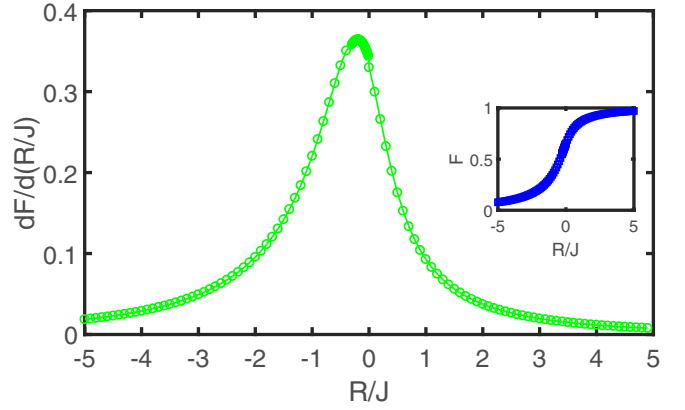

FIG. 7. First-order derivative of quantum fidelity per site $d(R/J)$ as a function of R/J for the spin-2 system. In the inset, the quantum fidelity is plotted.

$|\psi_G(R/J)\rangle$ is the ground-state wave function at R/J. With one of the biaxial spin nematic states as a reference state, the rapidity of the change occurring in the ground-state wave-function structure is to be the slope of the overlap function, i.e., the derivative of the overlap function with respect to the variable R/J. Recently, the fidelity susceptibility [89] has been used to estimate the crossover region in the BCS-BEC crossover. Without the loss of generality, we then consider the ground-state quantum fidelity per site $F(R/J)$ [78,90] given as $\ln F(R/J) = \lim_{L\to\infty} \ln f(\langle \psi_G(R/J)|\psi_G(+\infty) \rangle)/L$ in our iMPS framework. Figure 7 displays the first derivative of the quantum fidelity per site $F(R/J)$ as a function of R/J with the $F(R/J)$ in the inset. The most rapid change of the ground-state wave-function structure takes place with the value $dF/d(R/J) = 0.364$ at $R/J = -0.19$, as shown in Fig. 7. Then as a strict definition for quantum crossover region, one can choose the full width at half maximum of the peak in the derivative of quantum fidelity per site, i.e., as an example, $-1.21J \lesssim R_{cross} \lesssim 0.49J$ from Fig. 7. As one can confirm in Figs. 6(a) and 6(b), the quadrupole moments change relatively rapidly for the quantum crossover region estimated from the quantum fidelity. However, as a less-strict definition for quantum crossover region based on the significant changing behavior of the quadrupole moments, one can also choose the region in between the two uniaxial spin nematic points, i.e., $-R_a \lesssim R_{cross} \lesssim R_a$, as can be noticed in Fig. 6(b).

VI. SUMMARY

We have investigated quantum coherence in the ground state of infinite biquadratic spin-1 and -2 XY chains with rhombic single-ion anisotropy by employing the iMPS representation with the iTEBD method. The three quantum coherence measures such as the l_1 norm of coherence C_{l_1}, the relative entropy of coherence C_{re}, and the quantum Jensen-Shannon divergence C_{JS}, and the quantum mutual information have been calculated for the iMPS ground states. In fact, the spin-1 and -2 systems reveal very different features of quantum phases and phase transitions each other although their Hamiltonians have the same form in Eq. (1).

For the spin-1 system, all of the physical quantities including the ground-state energy, we have considered, have solidly captured the two discontinuous quantum phase transitions by means of their nonanalytical behaviors at the transition points $R = \pm R_c$. However, for the spin-2 system, the l_1 norm of coherence C_{l_1} and the quantum Jensen-Shannon divergence C_{JS} behave nonanalytically, which may indicate a phase transition similar to the case of the spin-1 system, at the vanishing rhombic-anisotropy point $R = 0$. Contrary to them, not only the relative entropy of coherence C_{re} and the mutual information I but also the ground-state energy do not show any nonanalytical behavior up to their second-order derivatives.

However, in our iMPS approach, the saturation behavior of the bipartite entanglement entropy with the increase of the truncation dimension χ manifests that the spin-2 system is not critical at $R = 0$, which rules out a possibility of occurring a continuous quantum phase transition. Accordingly, it was shown that the spin-2 system does undergo no explicit abrupt phase separation for the whole parameter space.

In order to determine the phases and the quantum phase transitions in the biquadratic spin-1 and -2 XY chains with rhombic single-ion anisotropy, the local magnetic moments and quadrupole moments have been investigated. We found that for the both spin-1 and -2 systems, the local magnetic moments are zero, i.e., $\langle S_i^\alpha \rangle = 0$ for the whole parameter space. For the spin-1 system, the local spin quadrupole order parameter $\langle Q_i^{x^2-y^2} \rangle$ characterize the three distinct uniaxial spin nematic phases by using the three different quadrupole orderings. Explicit discontinuous quantum phase transitions between the three uniaxial spin nematic phases have exhibited in the quadrupole order parameters.

In contrast to the spin-1 system, according to the sign change of the quadrupole order parameter $\langle Q_i^{x^2-y^2} \rangle$, the two biaxial nematic phases can be separated at the vanishing rhombic-anisotropy point $R = 0$ in the biquadratic spin-2 XY chain with rhombic single-ion anisotropy. As expected from the relative entropy of coherence C_{re} and the quantum mutual information I, no explicit phase transition between the two biaxial spin nematic phases was seen in the quadrupole order parameters. However, one biaxial spin nematic state is connected to the other biaxial spin nematic state by varying the system parameter through the vanishing rhombic-anisotropy point $R = 0$. Then this phase change can be called the quantum crossover, which was discussed by comparing with the explicit discontinuous phase transition in the Hamiltonian with $R = 0$. Furthermore, the quantum crossover region was estimated by using the quantum fidelity. As a result, in the sense that the quantum crossover between the two biaxial spin nematic phases does not undergo an abrupt change at a critical point, the relative entropy of coherence C_{re} and the quantum mutual information I exhibit a proper behavior without any abrupt change, while the l_1 norm of coherence C_{l_1} and the quantum Jensen-Shannon divergence C_{JS} disclose an unfaithful singular behavior of their first-order derivatives.

Finally, we summarize different features between the spin-1 and -2 systems. A remarkable difference between the spin-1 and -2 systems is the fact that the both spin-1 and spin-2 systems have the spin nematic phases but the nematic states are uniaxial for the spin-1 system and biaxial for the

spin-2 system. For the spin-2 system, the quantum crossover implies that one biaxial spin nematic state with local spin fluctuations along all axes can be gently varied to the other orthogonal biaxial spin nematic state through uniaxial spin nematic states by varying the rhombic single-ion anisotropy R inducing change of local spin fluctuations along all axes, as shown in Fig. 6(b). In contrast to the spin-2 system, for the spin-1 system, one uniaxial spin nematic state with local spin fluctuations in a characteristic plane is abruptly varied to the other orthogonal uniaxial spin nematic state with local spin fluctuations in an orthogonal plane to the characteristic plane by varying the rhombic single-ion anisotropy R. In this sense, another remarkable difference between the spin-1 and -2 systems is the uniaxial spin nematic phase in the parameter region $-R_c < R < R_c$ in between the other spin nematic phases for the spin-1 system, compared to the spin-2 system. This uniaxial spin nematic phase with the local spin
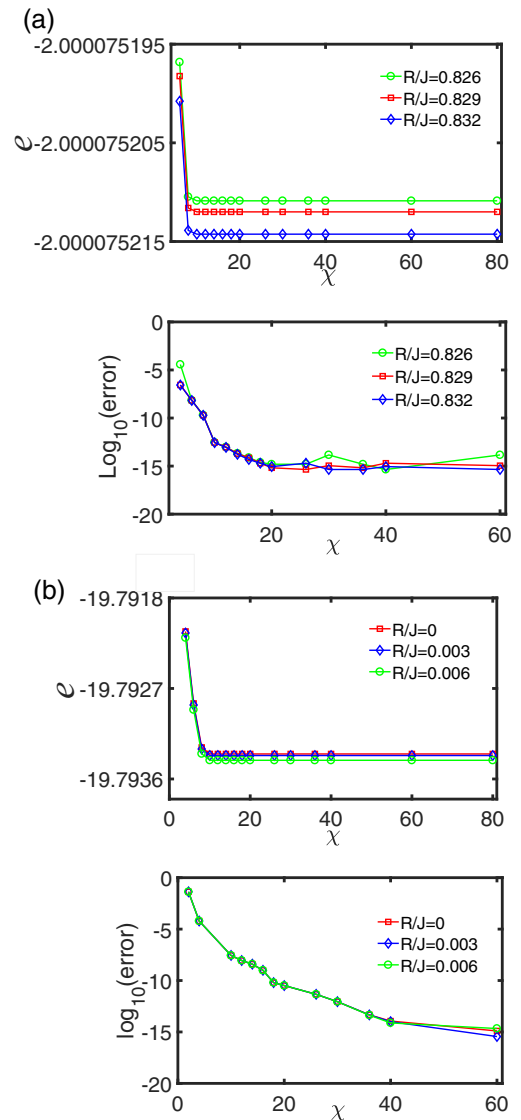

FIG. 8. Energy per site $e(\chi)$ and the relative error as a function of the truncation dimension χ for (a) the spin-1 and (b) the spin-2 systems.

fluctuation in the xy plane is in the product state of $|S^z = 0\rangle$, being an exact eigenstate of the Hamiltonian (1), and its characteristic features are $C_{l_1} = C_{re} = C_{JS} = I = \langle Q^{x^2-y^2} \rangle = 0$. At the corresponding point $R = 0$ of the spin-2 system characterized with $C_{l_1} = C_{re} = C_{JS} = \langle Q^{x^2-y^2} \rangle = 0$, the sharp contrast to the parameter region of the spin-1 system is the fact that the mutual information has the nonzero value and it is also maximum $I(R/J = 0) = I_{max}$ for the whole parameter range.

APPENDIX A: iMPS GROUND-STATE ENERGY

In our iMPS approach, the truncation dimension $\chi = 30$ was chosen because a higher truncation calculation does not change the physics we discussed in the main text. In this Appendix, we present the iMPS energy per site to show how the ground-state energy per site $e(\chi)$ changes with the truncation dimension χ. We choose the energy per site $e(\chi = 80)$ for the truncation dimension $\chi = 80$ as a reference value of energy

per site $e_{ref} \equiv e(\chi = 80)$. Thus we define the relative error as Error $(\chi) \equiv \text{abs}[(e(\chi) - e_{ref})/e_{ref}]$.

We plot the energy per site $e(\chi)$ and the relative error as a function of the truncation dimension χ for (a) the spin-1 and (b) the spin-2 systems in Fig. 8. For the both spin-1 and -2 systems, Fig. 8 shows that the iMPS energy per site $e(\chi)$ is readily saturated for the truncation dimension $\chi = 10$ with the relative error, Error $(\chi = 10) \sim 10^{-13}$ for the spin-1 system and Error $(\chi = 10) \sim 10^{-8}$ for the spin-2 system, where (a) for the spin-1 system, the reference energy per site are $e(\chi = 80) = -2.000075210876099$ for $R/J = 0.826$, $e(\chi = 80) = -2.002732436996759$ for $R/J = 0.829$, $e(\chi = 80) = -2.005390963256291$ for $R/J = 0.832$ and (b) for the spin-2 system, $e(\chi = 80) = -19.793351181555600$ for $R/J = 0$, $e(\chi = 80) = -19.793366930763035$ for $R/J = 0.003$, and $e(\chi = 80) = -19.793414177619063$ for $R/J = 0.006$.

For $\chi = 30$, the relative error reaches Error $(\chi = 30) \sim 10^{-15}$ for the spin-1 system and Error $(\chi = 30) \sim 10^{-13}$ for the spin-2 system.

APPENDIX B: EXACT DIAGONALIZATION CALCULATION

Our results based on the iMPS calculation can be confirmed by using an alternative numerical method, i.e., an
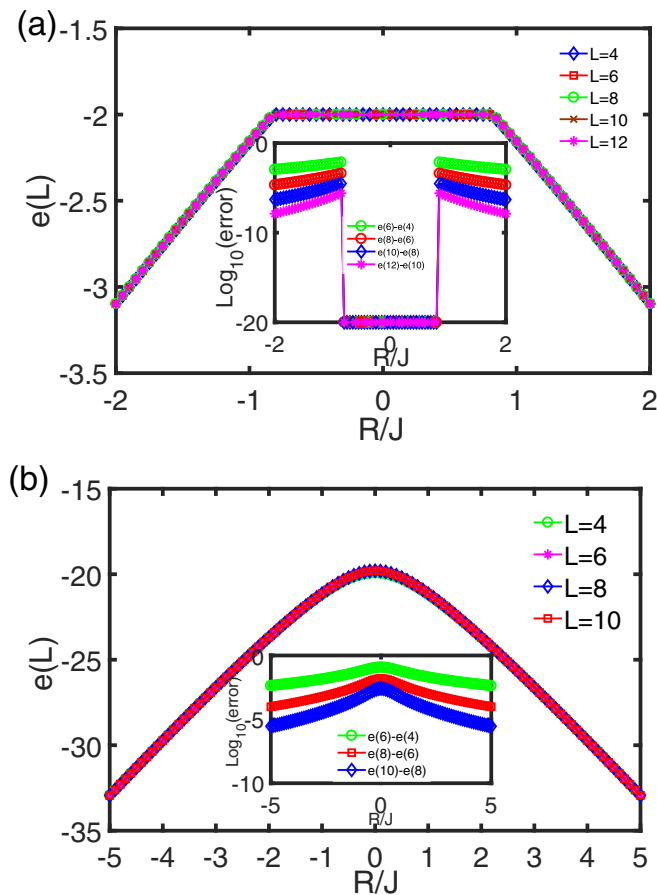

FIG. 9. Energy per site $e(\chi)$ as a function of the truncation dimension χ for (a) the spin-1 and (b) the spin-2 systems from the exact diagonalization. In the insets, the errors defined as error$(L) \equiv e(L) - e(L - 2)$ are presented, where L denotes the system size.
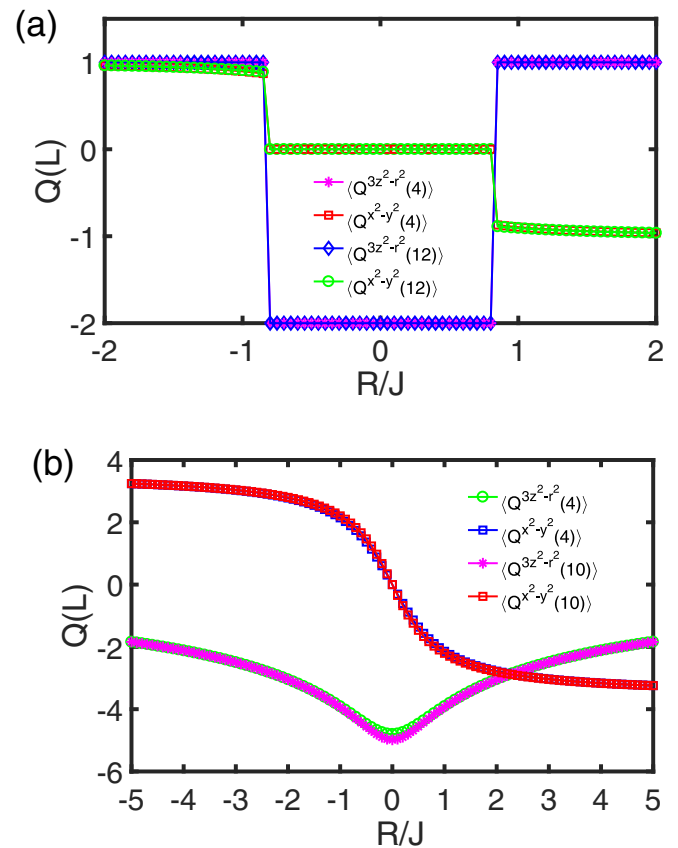

FIG. 10. Quadrupole order parameters $\langle Q^{x^2-y^2} \rangle$ and $\langle Q^{3z^2-r^2} \rangle$ as a function of R/J for (a) the spin-1 and the spin-2 systems from the exact diagonalization. For the spin-1 system, the system sizes $L = 4$ and 12 are considered. The system sizes $L = 4$ and 10 are considered for the spin-2 system.

exact diagonalization. In this Appendix, we will consider the finite lattice sizes of the Hamiltonian in Eq. (1). The finite-lattice-size biquadratic spin XY models with rhombic single-ion anisotropy can be described by using the Hamiltonian

$$H = -J \sum_{i=1}^{L} \left(S_i^x S_{i+1}^x + S_i^y S_{i+1}^y \right)^2 + R \sum_{i=1}^{L} \left[\left(S_i^x \right)^2 - \left(S_i^y \right)^2 \right],$$
(B1)

where the lattice chains consist of L spin-1 or -2 interacting spins. For the exact diagonalization, we consider the chains with the periodic boundary conditions.

Using the ground state obtained from the exact diagonalization, we plot the ground-state energy per site $e(L)$ as a function of R/J for the system size L in Fig. 9. The overall features of the energy are similar to those of the energy from the iMPS calculation in Fig. 3. In the insets, we present the difference between the energies, i.e., error $(L) \equiv e(L) - e(L-2)$. The insets show that the error (L) becomes smaller as the L increases.

For the spin-1 system, the energy per site $e(L)$ does not change much with respect to the system size L in the region $-R_c < R < R_c$ because the system is in a product state. Furthermore, one can easily notice the nonanalytic behaviors of

the energy at $R = \pm R_c$, which indicate the occurrences of the first-order phase transitions. For the spin-2 system, the energy does not exhibit any significant change at $R = 0$ as the system size L increases. Similarly to the iMPS calculation, any nonanalytic behavior of the energy is not observed for the spin-2 system.

From the exact diagonalization, we confirm that the magnetization is zero for the whole parameter range in the both spin-1 and -2 systems. Then in Fig. 10, we plot the quadrupole order parameters as a function of R/J in the cases of $L = 4$ and $L = 12$ for the spin-1 system and in the cases of $L = 4$ and $L = 10$ for the spin-2 system, respectively. Figure 10(a) for the spin-1 system shows that the quadrupole order parameter $\langle Q^{x^2-y^2} \rangle$ distinguishes the three spin nematic phases clearly, i.e., $\langle Q^{x^2-y^2} \rangle = 1$ for $R < -R_c$, $\langle Q^{x^2-y^2} \rangle = 0$ for $-R_c < R < R_c$, and $\langle Q^{x^2-y^2} \rangle = 1$ for $R > R_c$. This result is in agreement with the quadrupole order parameter from the iMPS calculation in Fig. 5. Also, Fig. 10(b) for the spin-2 system shows that $\langle Q^{x^2-y^2} \rangle > 0$ for $R < 0$, $\langle Q^{x^2-y^2} \rangle = 0$ for $R = 0$, and $\langle Q^{x^2-y^2} \rangle < 0$ for $R > 0$ in agreement with the iMPS calculation in Fig. 6(a). Consequently, it is shown that the results of the exact diagonalization and the iMPS calculations are in good agreement for the phase diagrams of the both spin-1 and -2 systems.

[1] S. Sachdev, *Quantum Phase Transitions* (Cambridge University Press, Cambridge, UK, 1999).

[2] U. Schollwöck, J. Richter, D. J. J. Farnell, and R. F. Bisho, *Quantum Magnetism* (Springer, New York, 2008).

[3] F. D. M. Haldane, Phys. Lett. A **93**, 464 (1983); Phys. Rev. Lett. **50**, 1153 (1983).

[4] F. Pollmann, E. Berg, A. M. Turner, and M. Oshikawa, Phys. Rev. B **85**, 075125 (2012).

[5] T. Tonegawa, K. Okamoto, H. Nakano, T. Sakai, K. Nomura, and M. Kaburagi, J. Phys. Soc. Jpn. **80**, 043001 (2011).

[6] K. Okamoto, T. Tonegawa, and T. Sakai, J. Phys. Soc. Jpn. **85**, 063704 (2016).

[7] Y.-C. Tzeng, Phys. Rev. B **86**, 024403 (2012).

[8] J. A. Kjäll, M. P. Zaletel, R. S. K. Mong, J. H. Bardarson, and F. Pollmann, Phys. Rev. B **87**, 235106 (2013).

[9] M. N. Barber and M. T. Batchelor, Phys. Rev. B **40**, 4621 (1989).

[10] A. Klümper, Europhys. Lett. **9**, 815 (1989); J. Phys. A **23**, 809 (1990).

[11] A. V. Chubukov, Phys. Rev. B **43**, 3337 (1991).

[12] G. Fáth and J. Sólyom, Phys. Rev. B **51**, 3620 (1995).

[13] M. Blume and Y. Y. Hsieh, J. Appl. Phys. **40**, 1249 (1969).

[14] N. Papanicolaou, Nucl. Phys. B **305**, 367 (1988).

[15] A. V. Chubukov, J. Phys.: Condens Matter **2**, 1593 (1990).

[16] R. Haramoto and J. Sak, Phys. Rev. B **46**, 8610 (1992).

[17] H. H. Chen and P. M. Levy, Phys. Rev. Lett. **27**, 1383 (1971).

[18] S. Nakatsuji, Y. Nambu, H. Tonomura, O. Sakai, S. Jonas, C. Broholm, H. Tsunetsugu, Y. Qiu, and Y. Maeno, Science **309**, 1697 (2005).

[19] D. Podolsky and E. Demler, New J. Phys. **7**, 59 (2005).

[20] H. Tsunetsugu and M. Arikawa, J. Phys. Soc. Jpn. **75**, 083701 (2006).

[21] S. Bhattacharjee, V. B. Shenoy, and T. Senthil, Phys. Rev. B **74**, 092406 (2006).

[22] A. Läuchli, F. Mila, and K. Penc, Phys. Rev. Lett. **97**, 087205 (2006).

[23] F. Michaud, F. Vernay, and F. Mila, Phys. Rev. B **84**, 184424 (2011).

[24] K. Harada and N. Kawashima, Phys. Rev. B **65**, 052403 (2002).

[25] T. A. Tóth, A. M. Läuchli, F. Mila, and K. Penc, Phys. Rev. B **85**, 140403(R) (2012),

[26] S.-S. Gong, W. Zhu, D. N. Sheng, and K. Yang, Phys. Rev. B **95**, 205132 (2017).

[27] H.-Y. Lee and N. Kawashima, Phys. Rev. B **97**, 205123 (2018).

[28] I. Niesen and P. Corboz, Phys. Rev. B **97**, 245146 (2018).

[29] Yu. A. Fridman, O. A. Kosmachev, A. K. Kolezhuk, and B. A. Ivanov, Phys. Rev. Lett. **106**, 097202 (2011).

[30] J. Stenger, S. Inouye, D. M. Stamper-Kurn, H.-J. Miesner, A. P. Chikkatur, and W. Ketterle, Nature (London) **396**, 345 (1998).

[31] D. M. Stamper-Kurn, M. R. Andrews, A. P. Chikkatur, S. Inouye, H.-J. Miesner, J. Stenger, and W. Ketterle, Phys. Rev. Lett. **80**, 2027 (1998).

[32] M. S. Chang, Q. Qin, W. Zhang, L. You, and M. S. Chapman, Nat. Phys. **1**, 111 (2005).

[33] A. Griesmaier, J. Werner, S. Hensler, J. Stuhler, and T. Pfau, Phys. Rev. Lett. **94**, 160401 (2005).

[34] M. Greiner, O. Mandel, T. Esslinger, T. W. Hänsch, and I. Bloch, Nature (Lond.) **415**, 39 (2002).

[35] J. L. Song, G. W. Semenoff, and F. Zhou, Phys. Rev. Lett. **98**, 160408 (2007).

[36] E. Demler and F. Zhou, Phys. Rev. Lett. **88**, 163001 (2002).

[37] F. Zhou and G. W. Semenoff, Phys. Rev. Lett. **97**, 180411 (2006).

[38] R. Barnett, A. Turner, and E. Demler, Phys. Rev. Lett. **97**, 180412 (2006).

[39] J.-S. Bernier, K. Sengupta, and Y. B. Kim, Phys. Rev. B **74**, 155124 (2006).

[40] H.-H. Tu, G.-M. Zhang, and L. Yu, Phys. Rev. B **74**, 174404 (2006).

[41] A. M. Turner, R. Barnett, E. Demler, and A. Vishwanath, Phys. Rev. Lett. **98**, 190404 (2007).

[42] P. Pfeuty, Ann. Phys. **57**, 79 (1970).

[43] M. M. Wolf, F. Verstraete, M. B. Hastings, and J. I. Cirac, Phys. Rev. Lett. **100**, 070502 (2008); See Eq. (5) for the relation between the two-point mutual information and the two-point correlations.

[44] B. Groisman, S. Popescu, and A. Winter, Phys. Rev. A **72**, 032317 (2005).

[45] C. Adami and N. J. Cerf, Phys. Rev. A **56**, 3470 (1997).

[46] F. C. Alcaraz and M. A. Rajabpour, Phys. Rev. B **91**, 155122 (2015).

[47] B. Schumacher and M. D. Westmoreland, Phys. Rev. A **74**, 042305 (2006).

[48] Y.-W. Dai, X.-H. Chen, S. Y. Cho, H.-Q. Zhou, and D.-X. Yao, arXiv:1805.03464 (2018).

[49] Y.-W. Dai, X.-H. Chen, S. Y. Cho, and H.-Q. Zhou, arXiv:2005.07924 (2020).

[50] T. Baumgratz, M. Cramer, and M. B. Plenio, Phys. Rev. Lett. **113**, 140401 (2014).

[51] J. Ma, B. Yadin, D. Girolami, V. Vedral, and M. Gu, Phys. Rev. Lett. **116**, 160407 (2016).

[52] A. Streltsov, U. Singh, H. S. Dhar, M. N. Bera, and G. Adesso, Phys. Rev. Lett. **115**, 020403 (2015).

[53] Z. Xi, Y. Li, and H. Fan, Sci. Rep. **5**, 10922 (2015).

[54] K. C. Tan, H. Kwon, C.-Y. Park, and H. Jeong, Phys. Rev. A **94**, 022329 (2016).

[55] W.-L. You, Y. Wang, T.-C. Yi, C. Zhang, and A. M. Oleś, Phys. Rev. B **97**, 224420 (2018).

[56] W. K. Wootters, Phys. Rev. Lett. **80**, 2245 (1998).

[57] Y. C. Li, J. Zhang, and H.-Q. Lin, Phys. Rev. B **101**, 115142 (2020).

[58] C. Radhakrishnan, I. Ermakov, and T. Byrnes, Phys. Rev. A **96**, 012341 (2017).

[59] J.-J. Chen, J. Cui, Y.-R. Zhang, and H. Fan, Phys. Rev. A **94**, 022112 (2016).

[60] G. Karpat, B. Çakmak, and F. F. Fanchini, Phys. Rev. B **90**, 104431 (2014).

[61] Q. Chen, G.-Q. Zhang, J.-Q. Cheng, and J.-B. Xu, Quant. Info. Proc. **18**, 8 (2019).

[62] T.-C. Yi, W.-L. You, N. Wu, and A. M. Oleś, Phys. Rev. B **100**, 024423 (2019).

[63] P. Thakur and P. Durganandini, Phys. Rev. B **102**, 064409 (2020).

[64] Y.-T. Sha, Y. Wang, Z.-H. Sun, and X.-W. Hou, Ann. Phys. **392**, 229 (2018).

[65] Y.-C. Li and H.-Q. Lin, Sci. Rep. **6**, 26365 (2016).

[66] M.-L. Hu, Y.-Y. Gao, and H. Fan, Phys. Rev. A **101**, 032305 (2020).

[67] A. L. Malvezzi, G. Karpat, B. Çakmak, F. F. Fanchini, T. Debarba, and R. O. Vianna, Phys. Rev. B **93**, 184428 (2016).

[68] R. Yu and Q. Si, Phys. Rev. Lett. **115**, 116401 (2015).

[69] Z. Wang, W.-J. Hu, and A. H. Nevidomskyy, Phys. Rev. Lett. **116**, 247203 (2016).

[70] H.-H. Lai, W.-J. Hu, E. M. Nica, R. Yu, and Q. Si, Phys. Rev. Lett. **118**, 176401 (2017).

[71] W.-J. Hu, S.-S. Gong, H.-H. Lai, H. Hu, Q. Si, and A. H. Nevidomskyy, Phys. Rev. B **100**, 165142 (2019).

[72] U. Schollwöck, T. Jolicoeur, and T. Garel, Phys. Rev. B **53**, 3304 (1996).

[73] Y. C. Tzeng, H. Onishi, T. Okubo, and Y. J. Kao, Phys. Rev. B **96**, 060404(R) (2017).

[74] J. Ren, Y. Wang, and W.-L. You, Phys. Rev. A **97**, 042318 (2018).

[75] G. Vidal, Phys. Rev. Lett. **91**, 147902 (2003).

[76] G. Vidal, Phys. Rev. Lett. **98**, 070201 (2007).

[77] Y. H. Su, S. Y. Cho, B. Li, H. L. Wang, and H. Q. Zhou, J. Phys. Soc. Jpn. **81**, 074003 (2012).

[78] Y. H. Su, B.-Q. Hu, S.-H. Li, and S. Y. Cho, Phys. Rev. E **88**, 032110 (2013).

[79] H.-T. Wang, B. Li, and S. Y. Cho, Phys. Rev. B **87**, 054402 (2013).

[80] Y.-W. Dai, S. Y. Cho, M. T. Batchelor, and H.-Q. Zhou, Phys. Rev. B **95**, 014419 (2017).

[81] L.-A. Wu, M. S. Sarandy, and D. A. Lidar, Phys. Rev. Lett. **93**, 250404 (2004).

[82] S. Rana, P. Parashar, and M. Lewenstein, Phys. Rev. A **93**, 012110 (2016).

[83] A. Osterloh, L. Amico, G. Falci, and R. Fazio, Nature (London) **416**, 608 (2002).

[84] L. Amico, R. Fazio, A. Osterloh, and V. Vedral, Rev. Mod. Phys. **80**, 517 (2008).

[85] V. E. Korepin, Phys. Rev. Lett. **92**, 096402 (2004).

[86] P. Calabrese and J. Cardy, J. Stat. Mech.: Theory Exp. (2004) P06002.

[87] L. Tagliacozzo, T. R. de Oliveira, S. Iblisdir, and J. I. Latorre, Phys. Rev. B **78**, 024410 (2008).

[88] K. Penc and A. Läuchli, in *Introduction to Frustrated Magnetism*, edited by C. Lacroix, P. Mendels, and F. Mila, Springer Series in Solid-State Sciences (Springer, Berlin, 2011).

[89] A. Khan and P. Pieri, Phys. Rev. A **80**, 012303 (2009).

[90] H.-Q. Zhou and J. P. Barjaktarevič, J. Phys. A: Math. Theor. **41**, 412001 (2008); H.-Q. Zhou, J.-H. Zhao, and B. Li, *ibid.* **41**, 492002 (2008).